International Journal of
Molecular Sciences

MDPI

Article

Aerobic Cytotoxicity of Aromatic *N*-Oxides: The Role of NAD(P)H:Quinone Oxidoreductase (NQO1)

Aušra Nemeikaitė-Čėnienė [1], Jonas Šarlauskas [2], Lina Misevičienė [2], Audronė Marozienė [2], Violeta Jonušienė [3], Mindaugas Lesanavičius [2] and Narimantas Čėnas [2,*]

1 State Research Institute Center for Innovative Medicine, Santariškių St. 5, LT-08406 Vilnius, Lithuania; ausra.ceniene@imcentras.lt
2 Institute of Biochemistry of Vilnius University, Saulėtekio 7, LT-10257 Vilnius, Lithuania; jonas.sarlauskas@bchi.vu.lt (J.Š.); lina.miseviciene@bchi.vu.lt (L.M.); audrone.maroziene@bchi.vu.lt (A.M.); mindaugas.lesanavicius@gmail.com (M.L.)
3 Institute of Biosciences of Vilnius University, Saulėtekio 7, LT-10257 Vilnius, Lithuania; violeta.jonusiene@gf.vu.lt
* Correspondence: narimantas.cenas@bchi.vu.lt; Tel.: +370-5-223-4392

Received: 20 October 2020; Accepted: 18 November 2020; Published: 19 November 2020

Abstract: Derivatives of tirapazamine and other heteroaromatic *N*-oxides (ArN→O) exhibit tumoricidal, antibacterial, and antiprotozoal activities, which are typically attributed to bioreductive activation and free radical generation. In this work, we aimed to clarify the role of NAD(P)H:quinone oxidoreductase (NQO1) in ArN→O aerobic cytotoxicity. We synthesized 9 representatives of ArN→O with uncharacterized redox properties and examined their single-electron reduction by rat NADPH:cytochrome P-450 reductase (P-450R) and *Plasmodium falciparum* ferredoxin:$NADP^+$ oxidoreductase (*Pf*FNR), and by rat NQO1. NQO1 catalyzed both redox cycling and the formation of stable reduction products of ArN→O. The reactivity of ArN→O in NQO1-catalyzed reactions did not correlate with the geometric average of their activity towards P-450R- and *Pf*FNR, which was taken for the parameter of their redox cycling efficacy. The cytotoxicity of compounds in murine hepatoma MH22a cells was decreased by antioxidants and the inhibitor of NQO1, dicoumarol. The multiparameter regression analysis of the data of this and a previous study (DOI: 10.3390/ijms20184602) shows that the cytotoxicity of ArN→O (n = 18) in MH22a and human colon carcinoma HCT-116 cells increases with the geometric average of their reactivity towards P-450R and *Pf*FNR, and with their reactivity towards NQO1. These data demonstrate that NQO1 is a potentially important target of action of heteroaromatic *N*-oxides.

Keywords: tirapazamine; reductive activation; NAD(P)H:quinone oxidoreductase; oxidative stress; cytotoxicity

1. Introduction

N-oxides of 1,2,4-benzotriazine, quinoxaline, and phenazine (ArN→O) possess promising antitumor, antiprotozoal, and antibacterial activities, including their potential application as hypoxia-specific antitumor agents ([1–6], and references therein). In most cases, their action is attributed to the enzymatic reduction and free radical generation. Among their representatives, the reactions of 3-amino-1,2,4-benzotriazine-1,4-dioxide (tirapazamine, TPZ) and its derivatives have been studied most comprehensively. TPZ (**a**) is enzymatically reduced in a single-electron way to a free radical (**b**), which forms DNA-damaging species under hypoxic conditions, namely, an oxidizing hydroxyl radical ($OH^·$) ([2,7,8], and references therein), and/or a highly reactive benzotriazinyl radical (**c**) that abstracts a hydrogen atom from DNA ([9,10], and references therein (Scheme 1). The nature of DNA-damaging species remains a matter of debate. The final relatively nontoxic metabolites of TPZ

are its mono-*N*-oxide (**d**), formed possibly via free radical (**c**) intermediate, and its nor-oxide (**f**) [2,7,11]. Their formation is strongly inhibited under aerobic conditions.

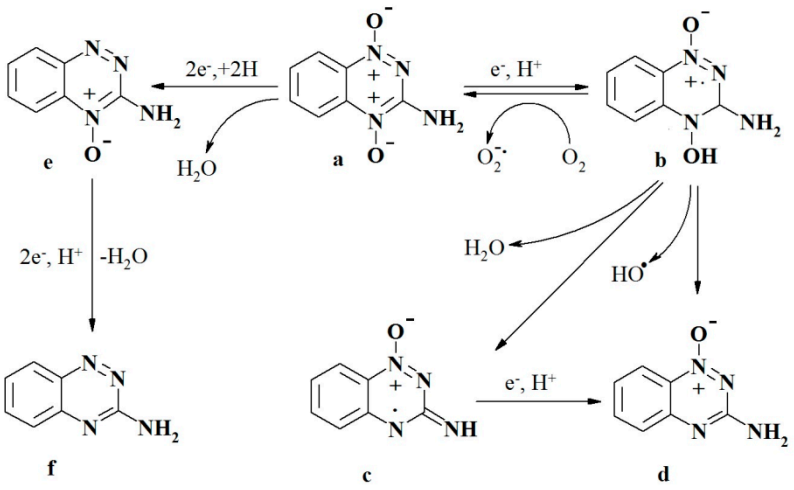

Scheme 1. Pathways of the reduction of tirapazamine in the cell.

The aerobic cytotoxicity of ArN→O is typically attributed to their redox cycling (Scheme 1), leading to the formation of superoxide (O_2^-) and subsequent oxidative stress [1,2]. This phenomenon deserves certain interest because some TPZ analogs possess anticancer activity at micromolar concentrations even under oxic conditions [12–14], and/or are toxic to normal tissues [15]. Besides, the oxidative stress-type mammalian cell cytotoxicity may be important as a side effect in the antimicrobial and antiparasitic action of ArN→O ([2,6], and references therein). Flavoenzyme NADPH:cytochrome P-450 reductase (P-450R) and/or insufficiently characterized intranuclear NAD(P)H-oxidizing flavoenzymes are assumed to be mainly responsible for the single-electron reduction of ArN→O irrespectively of hypoxic or oxic conditions ([16,17], and references therein). Another enzyme, potentially relevant to the cytotoxicity of ArN→O, is NAD(P)H:quinone oxidoreductase (NQO1, DT-diaphorase). NQO1 is a dimeric enzyme containing one molecule of FAD per subunit, located mainly in the cytosol [18]. It reduces quinones and nitroaromatic compounds in an obligatory two-electron way ([19,20], and references therein), and is considered to be a target of bioreductively-activated quinone antitumor agents [21]. NQO1 reduces TPZ and its derivatives much slower than quinones in a mixed single- and the two-electron way [22]. The data on the impact of NQO1 on cytotoxicity of TPZ are controversial [22–25]. However, the studies of its reactions with ArN→O deserve certain interest because the activity of NQO1 is frequently elevated in various tumors ([26], and references therein).

The aerobic cytotoxicity of several ArN→O in MH22a mouse hepatoma cells roughly increased with their single-electron reduction midpoint potential (E^1_7) [22], which demonstrates an involvement of P-450R and/or other single-electron transferring flavoenzymes. In parallel, the cytotoxicity was decreased by dicoumarol, which points to the possible participation of NQO1 in cytotoxic events. In this work, we extended these studies using a series of previously unexplored aromatic *N*-oxides and have shown that NQO1 unequivocally contributes to the cytotoxicity of ArN→O.

2. Results

2.1. Reactions of Aromatic N-Oxides with Flavoenzymes Dehydrogenases-Electrontransferases

Previously we studied the enzymatic reactions and cytotoxicity of a number of ArN→O, mostly 7-substituted tirapazamine derivatives, whose E^1_7 varied between −0.318 V and −0.575 V [22]. In this work, we extended these studies using representatives of several groups of ArN→O with uncharacterized values of E^1_7 (Figure 1).

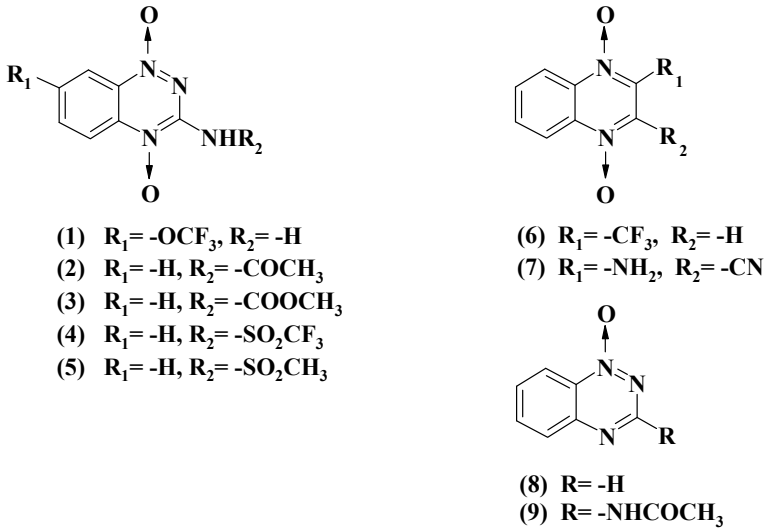

Figure 1. Formulae of heteroaromatic *N*-oxides used in this work: derivatives of tirapazamine (**1**–**5**), quinoxaline-1,4-dioxide (**6**,**7**), and 1,2,4-benzotriazine-1-oxide (**8**,**9**).

Table 1 contains bimolecular rate constants (k_{cat}/K_m) of reduction of examined ArN→O by P-450R and *Plasmodium falciparum* ferredoxin:NADP$^+$ oxidoreductase (*Pf*FNR), which was used as a model single-electron transferring enzyme [27]. For the most active oxidants of P-450R studied in this work, 7-CF_3O-tirapazamine, and 3-CH_3CONH- and 3-CH_3OCONH-substituted 1,2,4-benzotriazine-1,4-dioxides (Table 1), the k_{cat} at their saturated concentrations were in the range of 16.0–18.0 s^{-1}, i.e., close to 50% of the rate of cytochrome *c* reduction by P-450R. The above compounds were also the most active oxidants of *Pf*FNR (Table 1), with k_{cat} of their reduction reaching 11.0–13.0 s^{-1}. In other cases, the reaction rates were proportional to the concentration of compounds up to the limits of their solubility, 300–600 μM. Because *Pf*FNR does not reduce cytochrome *c* directly [27], it was possible to demonstrate the redox cycling of synthesized ArN→O monitoring the reduction of cytochrome *c* added to the reaction mixture. The rates of this reaction were equal to 175–190% NADPH oxidation rate. The cytochrome *c* reduction was inhibited by 20–40% by 100 U/mL superoxide dismutase (SOD), which points to the formation of superoxide.

Typically, the logarithms of k_{cat}/K_m of single-electron reduction of ArN→O by flavoenzymes dehydrogenases-electrontransferases such as P-450R or *Pf*FNR linearly increase with E^1_7 [22,27]. This is attributed to an "outer-sphere" electron transfer mechanism, where the reactivity of compounds is insignificantly influenced by their structural peculiarities [28]. Therefore, log k_{cat}/K_m of homologous oxidants in single-electron enzymatic reduction reaction may serve as the parameter characterizing their E^1_7, i.e., the energetic of single-electron reduction. The use of the geometric average of k_{cat}/K_m obtained in several enzymatic systems improves the prediction accuracy [29,30]. Table 1 contains the logarithms of geometric averages of k_{cat}/K_m of ArN→O in P-450R- and *Pf*FNR-catalyzed reactions (log k_{cat}/K_m (avge) = 0.5 log k_{cat}/K_m (P-450R) + 0.5 log k_{cat}/K_m (*Pf*FNR)). For comparison, the reduction rate constants of compounds **10**–**18** obtained in our previous studies [22,27] are also presented (Table 1). The log k_{cat}/K_m (avge) of these compounds correlates well with their E^1_7 values:

$$\log k_{cat}/K_m \text{ (avge)} = (7.23 \pm 0.29) + (6.96 \pm 0.65)\, E^1_7,\ r^2 = 0.9430. \quad (1)$$

A similar correlation is obtained including the assumed E^1_7 values for compounds **6**,**8** (Table 1):

$$\log \text{kcat/Km (avge)} = (7.24 \pm 0.27) + (6.97 \pm 0.59)\ \text{E17, r2} = 0.9400. \quad (2)$$

For compounds with unavailable E^1_7 values, the introduction of electron-accepting substituents into 3-NH_2 group or into 7- or 2-positions of the aromatic system in most cases increased their log

k_{cat}/K_m (avge) as compared with parent compounds (Table 1). Therefore, in this case, log k_{cat}/K_m (avge) appears to be a suitable parameter describing the ease of single-electron reduction of ArN→O.

Table 1. The single-electron reduction midpoint potentials (E^1_7) of aromatic *N*-oxides, the steady-state bimolecular rate constants (k_{cat}/K_m) of their reduction by P-450R and *Pf*FNR, and the logs of the geometric averages of their reactivity (log k_{cat}/K_m (avge)).

No.	Compound	E^1_7 (V) [a]	k_{cat}/K_m ($M^{-1}\cdot s^{-1}$)		log k_{cat}/K_m (avge)
			P-450R	*Pf*FNR	
1	7-CF_3O-tirapazamine		$4.6 \pm 0.4 \times 10^4$	$3.8 \pm 0.4 \times 10^4$	4.62
2	3-CH_3CONH-1,2,4-benzotriazine-1,4-dioxide		$7.0 \pm 0.5 \times 10^4$	$6.2 \pm 0.5 \times 10^4$	4.82
3	3-CH_3OCONH-1,2,4-benzotriazine-1,4-dioxide		$8.0 \pm 0.9 \times 10^4$	$4.8 \pm 0.4 \times 10^4$	4.78
4	3-CF_3SO_2NH-1,2,4-benzotriazine-1,4-dioxide		$2.5 \pm 0.3 \times 10^4$	$2.6 \pm 0.3 \times 10^4$	4.41
5	3-CH_3SO_2NH-1,2,4-benzotriazine-1,4-dioxide		$2.7 \pm 0.3 \times 10^3$	$7.9 \pm 0.5 \times 10^3$	3.67
6	2-CF_3-quinoxaline-1,4-dioxide	(−0.465) [b]	$2.7 \pm 0.3 \times 10^4$	$8.9 \pm 0.7 \times 10^3$	4.19
7	2-NH_2-3-CN-quinoxaline-1,4-dioxide		$4.7 \pm 0.4 \times 10^3$	$1.8 \pm 0.2 \times 10^4$	3.96
8	1,2,4-Benzotriazine-1-oxide	(−0.431) [b]	$1.7 \pm 0.2 \times 10^4$	$4.3 \pm 0.3 \times 10^3$	3.94
9	3-CH_3CONH-1,2,4-benzotriazine-1-oxide		$8.7 \pm 0.9 \times 10^3$	$1.6 \pm 0.1 \times 10^3$	3.58
	ArN→O with available E^1_7 values				
10	1,2,4-Benzotriazine-1,4-dioxide	−0.318	$4.3 \pm 0.4 \times 10^5$ [c]	$2.5 \pm 0.3 \times 10^4$	5.00
11	7-CF_3-tirapazamine	−0.345	$8.7 \pm 0.7 \times 10^4$ [c]	$5.2 \pm 0.4 \times 10^4$ [d]	4.83
12	7-Cl-tirapazamine	−0.400	$6.9 \pm 0.7 \times 10^4$ [c]	$3.7 \pm 0.4 \times 10^4$ [d]	4.71
13	7-F-tirapazamine	−0.400	$3.4 \pm 0.3 \times 10^4$ [c]	$2.7 \pm 0.2 \times 10^4$ [d]	4.48
14	Tirapazamine	−0.455	$1.1 \pm 0.1 \times 10^4$ [c]	$4.4 \pm 0.5 \times 10^3$ [d]	3.84
15	7-CH_3-tirapazamine	−0.474	$8.6 \pm 0.7 \times 10^3$ [c]	$5.0 \pm 0.6 \times 10^3$ [d]	3.82
16	7-C_2H_5O-tirapazamine	−0.494	$4.5 \pm 0.5 \times 10^3$ [c]	$4.5 \pm 0.5 \times 10^3$ [d]	3.65
17	3-Amino-1,2,4-benzotriazine-1-oxide	−0.568	$2.8 \pm 0.2 \times 10^3$ [c]	$3.2 \pm 0.2 \times 10^3$ [d]	3.48
18	Quinoxaline-1,4-dioxide	−0.575	$3.3 \pm 0.2 \times 10^3$ [c]	$8.2 \pm 0.9 \times 10^2$ [d]	3.22

[a] E^1_7 of compounds taken from Ref. [7,31,32], [b] Calculated using the E^1_7 differences between compounds **11** and **14**, 0.110 V, and compounds **17** and **14**, −0.113 V, respectively, [c] Taken from Ref. [22], [d] Taken from Ref. [27].

2.2. NQO1-Catalyzed Reduction of Aromatic N-Oxides

NQO1 performs a slow reduction of ArN→O [22,33]. The reactivity of compounds **1**–**9** determined in this work was similar to that of compounds **10**–**18** [22], except for its larger variation (Table 2). The log k_{cat}/K_m for compounds **1**–**18** (Table 2) does not correlate with the energetics of their single-electron reduction, because of its dependence on E^1_7 or log k_{cat}/K_m (avge) is described by $r^2 = 0.0451$ and $r^2 = 0.1441$, respectively. Because the reactivity of quinones towards NQO1 depends on their van der Waals volume (VdWvol) [19], we also used this parameter for calculations (Table 2). However, the combined use of log k_{cat}/K_m (avge) and VdWvol or VdWvol + $(VdWvol)^2$ as independent variables also did not give satisfactory results, being described by $r^2 = 0.2302$ and $r^2 = 0.3846$, respectively. Thus, the structural requirements for the fast reduction of ArN→O by NQO1 remain unclear at this time.

Under anaerobic conditions, NQO1 reduces TPZ into its 4-monoxide (**d**) and nor-oxide (**f**) (Scheme 1) [33]. The reduction is strongly inhibited by O_2 [33] and is accompanied by redox cycling process [22]. Because of the low rate of this reaction, we selected more reactive 3-CH_3CONH-1,2,4-benzotriazine-1,4-dioxide (**2**) (Table 2) for subsequent studies. The temperature dependence of k_{cat}/K_m of reaction determined according to NADPH oxidation in the absence of activators gives the activation enthalpy ($\Delta H^{\neq}$) of 37.76 ± 1.93 kJ mol^{-1} and the activation entropy ($\Delta S^{\neq}$) of -42.97 ± 6.68 J mol^{-1} K^{-1}. In the presence of the NADPH regeneration system under aerobic conditions, the disappearance of compound absorbance at 427 nm is accompanied by absorbance rise at 375 nm (Figure 2A). This shows that the possible reaction product is CH_3CONH-1,2,4-benzotriazine-1-oxide (**9**) (Figure 1), which possesses absorbance maximum at this wavelength (data not shown). The more detailed characterization of reaction products is beyond the scope of the present work.

Table 2. The steady-state rate constants of reduction of aromatic *N*-oxides by NQO1 and their calculated van der Waals volumes (VdWvol).

No.	Compound	k_{cat} (s^{-1})	k_{cat}/K_m ($M^{-1}\cdot s^{-1}$)	VdWvol ($Å^3$) [a]
1	7-CF_3O-tirapazamine	0.11 ± 0.02	$1.6 \pm 0.1 \times 10^3$	175.8
2	3-CH_3CONH-1,2,4-benzotriazine-1,4-dioxide	3.40 ± 0.20 3.00 ± 0.20 [b]	$1.3 \pm 0.1 \times 10^4$ $1.0 \pm 0.1 \times 10^4$ [b]	172.3
3	3-CH_3OCONH-1,2,4-benzotriazine-1,4-dioxide	2.40 ± 0.22	$3.0 \pm 0.2 \times 10^3$	180.7
4	3-CF_3SO_2NH-1,2,4-benzotriazine-1,4-dioxide	0.34 ± 0.06	$1.0 \pm 0.2 \times 10^3$	203.5
5	3-CH_3SO_2NH-1,2,4-benzotriazine-1,4-dioxide	0.40 ± 0.05	$1.2 \pm 0.2 \times 10^3$	184.9
6	2-CF_3-quinoxaline-1,4-dioxide	13.5 ± 1.72	$2.4 \pm 0.2 \times 10^4$	168.2
7	2-NH_2-3-CN-quinoxaline-1,4-dioxide	0.11 ± 0.02	$1.4 \pm 0.1 \times 10^3$	146.2
8	1,2,4-Benzotriazine-1-oxide	1.10 ± 0.12	$2.1 \pm 0.2 \times 10^3$	111.7
9	3-CH_3CONH-1,2,4-benzotriazine-1-oxide	0.06 ± 0.02	$5.0 \pm 1.0 \times 10^2$	163.5
10	1,2,4-Benzotriazine-1,4-dioxide [c]	1.00 ± 0.10	$5.1 \pm 0.7 \times 10^3$	120.5
11	7-CF_3-tirapazamine [c]	1.30 ± 0.10	$3.7 \pm 0.4 \times 10^3$	167.0
12	7-Cl-tirapazamine [c]	1.00 ± 0.10	$4.3 \pm 0.4 \times 10^3$	152.6
13	7-F-tirapazamine [c]	0.70 ± 0.10	$4.9 \pm 0.6 \times 10^3$	143.5
14	Tirapazamine [c]	0.20 ± 0.10	$2.4 \pm 0.2 \times 10^3$	131.5
15	7-CH_3-tirapazamine [c]	0.30 ± 0.05	$1.7 \pm 0.1 \times 10^3$	148.8
16	7-C_2H_5O-tirapazamine [c]	0.30 ± 0.04	$1.0 \pm 0.1 \times 10^3$	174.9
17	3-Amino-1,2,4-benzotriazine-1-oxide [c]	0.10 ± 0.02	$1.6 \pm 0.2 \times 10^3$	122,7
18	Quinoxaline-1,4-dioxide [c]	0.60 ± 0.10	$7.9 \pm 0.9 \times 10^3$	126.8

[a] Calculated according to [34], [b] Determined in the absence of activators, [c] Taken from Ref. [22].

The data of Figure 2B show that the rate of 3-CH_3CONH-1,2,4-benzotriazine-1,4-dioxide disappearance was equal to 70–75% NADPH oxidation rate determined in the absence of NADPH regeneration system. The rate of compound disappearance was directly proportional to NQO1 concentration in the range of 12.5–100 nM. The reaction was accompanied by the reduction of added cytochrome *c* with the rate being equal to 30–35% NADPH oxidation rate (Figure 2B). The reduction of cytochrome *c* was partly inhibited by superoxide dismutase, which demonstrates the formation of O_2^-. During the reduction of (**2**) by *Pf*FNR, the rate of added cytochrome *c* reduction was much higher, being equal to 180–190% NADPH oxidation rate. The cytochrome *c* reduction was inhibited by SOD by 20%.

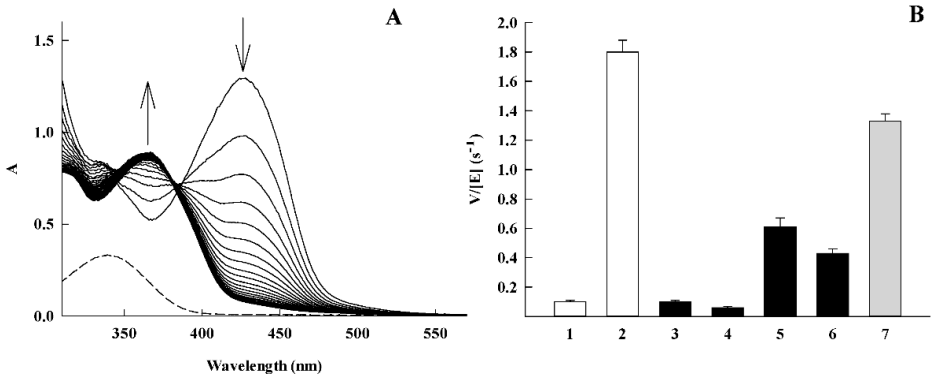

Figure 2. Reduction of 3-CH_3CONH-1,2,4-benzotriazine-1,4-dioxide (**2**) by NAD(P)H:quinone oxidoreductase (NQO1). (**A**) The spectral changes of 200 μM (**2**) in the presence of 50 nM NQO1, and 50 μM NADPH and NADPH regeneration system. The absorbance of NADPH is shown by a dashed line. The scans are recorded each 15 min. (**B**) The rates of NQO1-catalyzed oxidation of NADPH (1,2), reduction of cytochrome *c* (3–6), and depletion of 200 μM (**2**) in the presence of 200 μM NADPH (7). Additions: NADPH (1), NADPH + (**2**) (2,7), NADPH + cytochrome *c* (3), NADPH + cytochrome *c* + 100 U/mL SOD (4), NADPH + (**2**) + cytochrome *c* (5), NADPH + (**2**) + cytochrome *c* + SOD (6), $n = 3$, $p < 0.01$ for 3 against 4 and for 5 against 6.

2.3. Cytotoxicity of Aromatic N-Oxides

In cytotoxicity studies, we determined the concentrations of ArN→O for 50% cell survival (cL_{50}) in murine hepatoma MH22a cells and their concentrations for 50% of maximal inhibition (GI_{50}) of the proliferation of human colon adenocarcinoma HCT-116 cells (Table 3). The data of our previous study [22] are also presented for comparison.

Table 3. The logarithms of the geometric averages of ArN→O reactivity in P450R- and *Pf*FNR-catalyzed reactions (log k_{cat}/K_m (avge)), their octanol/water distribution coefficients at pH 7.0 (log *D*), their concentrations for 50% cell survival (cL_{50}) in murine hepatoma MH22a cells, and their concentrations causing 50% maximal proliferation inhibition (GI_{50}) of human colon carcinoma HCT-116 cells.

No.	Compound	log k_{cat}/K_m (avge)	log *D*	cL_{50} (μM) MH22a	GI_{50} (μM) HCT-116
1	7-CF_3O-tirapazamine	4.62	1.32	3.6 ± 0.7	17 ± 3.0
2	3-CH_3CONH-1,2,4-benzotriazine-1,4-dioxide	4.82	−0.82	1.5 ± 0.3	2.5 ± 0.5
3	3-CH_3OCONH-1,2,4-benzotriazine-1,4-dioxide	4.78	−0.08	9.4 ± 1.4	6.3 ± 1.0
4	3-CF_3SO_2NH-1,2,4-benzotriazine-1,4-dioxide	4.41	−0.40	44 ± 6.5	125 ± 19
5	3-CH_3SO_2NH-1,2,4-benzotriazine-1,4-dioxide	3.67	−2.42	184 ± 25	185 ± 23
6	2-CF_3-quinoxaline-1,4-dioxide	4.19	0.42	10 ± 2.0	12.5 ± 2.0
7	2-NH_2-3-CN-quinoxaline-1,4-dioxide	3.96	−0.18	358 ± 52	125 ± 17
8	1,2,4-Benzotriazine-1-oxide	3.94	0.45	168 ± 21	225 ± 27
9	3-CH_3CONH-1,2,4-benzotriazine-1-oxide	3.58	0.37	≥600	≥1000
10	1,2,4-Benzotriazine-1,4-dioxide	5.00	−0.70	11 ± 1.5 [a]	18 ± 2.0
11	7-CF_3-tirapazamine	4.83	0.76	3.4 ± 0.4 [a]	6.0 ± 1.0 [a]
12	7-Cl-tirapazamine	4.71	0.49	3.1 ± 0.5 [a]	13 ± 1.5 [a]
13	7-F-tirapazamine	4.48	0.03	7.2 ± 1.0 [a]	25 ± 4.0
14	Tirapazamine	3.84	0.11	31 ± 5.5 [a] 28 ± 4.0	75 ± 7.0 [a] 64 ± 7.0
15	7-CH_3-tirapazamine	3.82	0.40	83 ± 10 [a]	50 ± 6.0 [a]
16	7-C_2H_5O-tirapazamine	3.65	0.08	64 ± 10 [a]	60 ± 7.0 [a]
17	3-Amino-1,2,4-benzotriazine-1-oxide	3.48	0.30	≥600 [a]	≥600 [a]
18	Quinoxaline-1,4-dioxide	3.22	−0.90	325 ± 40 [a]	≥800

[a] Taken from Ref. [22].

We previously demonstrated the prooxidant character of cytotoxicity of ArN→O in MH22a cells [22]. In line with this, the cytotoxicity of several randomly selected ArN→O explored in this work, was decreased by desferrioxamine (DESF) and the antioxidant *N*,*N*′-diphenyl-*p*-phenylenediamine (DPPD), and enhanced by 1,3-bis(2-chloroethyl)-1-nitrosourea (BCNU), the latter inactivating glutathione reductase and depleting reduced glutathione [35] (Table 4). Besides, their cytotoxicity was decreased by an inhibitor of NQO1, dicoumarol (DIC) (Table 4).

Table 4. Modulation of the cytotoxicity of aromatic *N*-oxides in MH22a cells by desferrioxamine (DESF), *N*,*N*′-diphenyl-*p*-phenylenediamine (DPPD), 1,3-bis(2-chloroethyl)-1-nitrosourea (BCNU), and dicoumarol (DIC). The additions of compounds did not affect the cell viability in control experiments, 98.5–99.3%, $n = 3$, * $p < 0.05$, ** $p < 0.02$, *** $p < 0.01$.

No.	Compound	Cell Viability (%)				
		No Additions	Additions:			
			DESF (1.0 mM)	DPPD (2.5 μM)	BCNU (20 μM)	DIC (20 μM)
1	3-CH_3CONH-1,2,4-benzotriazine-1,4-dioxide, 1.5 μM	47.2 ± 4.0	71.8 ± 4.0 ***	64.9 ± 3.8 ***	34.0 ± 3.0 **	83.7 ± 6.1 ***
2	2-NH_2-3-CN-quinoxaline-1,4-dioxide, 350 μM	47.3 ± 4.2	83.5 ± 7.0 **	72.1 ± 5.7 **	35.3 ± 3.6 *	71.6 ± 5.1 **
3	1,2,4-Benzotriazine-1,4-dioxide, 10 μM	55.6 ± 4.5	n.d.	n.d.	n.d.	81.2 ± 7.4 **
4	3-CF_3SO_2NH-1,2,4-benzotriazine-1,4-dioxide, 40 μM	55.8 ± 4.9	n.d.	n.d.	n.d.	79.0 ± 3.1 **
5	2-CF_3-quinoxaline-1,4-dioxide, 10 μM	57.6 ± 4.5	n.d.	n.d.	n.d.	83.1 ± 5.6 **

In quantitative analysis of cytotoxicity of ArN→O, we used the ease of their single-electron reduction (log k_{cat}/K_m (avge), Table 1), lipophilicity (log *D*, Table 3)), and reactivity towards NQO1

(log k_{cat}/K_m (NQO1), Table 2) as the correlation parameters. The data were analyzed using the linear multiparameter regression:

$$\log cL_{50} \text{ (or } \log GI_{50}) = a + b \log k_{cat}/K_m \text{ (avge)} + c \log D + d \log k_{cat}/K_m \text{ (NQO1)} \quad (3)$$

The calculated coefficients in Equation (3) (Table 5) show that the cytotoxicity of compounds in both cell lines roughly increases with their log k_{cat}/K_m (avge) when it is used as a single variable. The introduction of log k_{cat}/K_m (NQO1) as a second variable improved the correlations, and also unequivocally demonstrated that the ArN→O cytotoxicity increases with their reactivity towards NQO1 (Table 5).

Table 5. The results of the multiparameter analysis of ArN→O cytotoxicity (Table 3) according to Equation (3).

Cell Line	*a*	*b*	*c*	*d*	r^2
MH22a	7.22 ± 0.80	−1.36 ± 0.19	-	-	0.7638
	7.07 ± 0.84	−1.33 ± 0.20	−0.09 ± 0.13	-	0.7704
	8.44 ± 0.88	−1.20 ± 0.18	-	−0.55 ± 0.24	0.8266
	8.30 ± 0.88	−1.14 ± 0.19	−0.13 ± 0.118	−0.59 ± 0.24	0.8405
HCT-116	6.68 ± 0.73	−1.19 ± 0.17	-	-	0.7440
	6.63 ± 0.79	−1.18 ± 0.19	−0.03 ± 0.13	-	0.7448
	7.74 ± 0.82	−1.05 ± 0.17	-	−0.48 ± 0.22	0.8052
	7.67 ± 0.85	−1.02 ± 0.18	−0.06 ± 0.11	−0.50 ± 0.23	0.8093

In all cases (Table 5), the coefficient *d* characterizing an involvement of NQO1 (Equation (3)) is statistically significant ($p < 0.05$). The use of log *D* as an additional variable did not improve the correlations and demonstrated a limited impact of lipophilicity on ArN→O cytotoxicity (Table 5), which is similar to the data of a previous study [31].

The role of NQO1 in the cytotoxicity of ArN→O was additionally assessed using bovine leukemia virus-transformed lamb embryo kidney fibroblasts (line FLK [36]), murine embryonic liver cells (line BNL CL.2 [37]), and primary mice splenocytes [38] (Supplemental Information, Table S1). In this case, DIC protected against the cytotoxicity of TPZ and 3-CH_3CONH-1,2,4-benzotriazine-1,4-dioxide in cell lines with a relatively high content of NQO1, but did not protect against their cytotoxicity in mice splenocytes with low NQO1 content, 4.0 nmol cytochrome *c* reduced × min^{-1} × mg^{-1} [38] (Table S2).

3. Discussion

In this study, we examined the relationship between enzymatic redox properties and aerobic cytotoxicity of aromatic *N*-oxides with a particular emphasis on the role of NQO1. The rate constants of single-electron reduction of ArN→O **1–9** by P-450R and *Pf*FNR (Table 1) are in line with previous findings [22,27], showing that the reactivity is mostly determined by the electron-accepting potency of ArN→O, and hardly depend on their structural peculiarities. Their log k_{cat}/K_m (avge) proved to be a reasonable substitute for E^1_7 because of their good interrelationship (Equations (1) and (2)). Interestingly, its use for the description of ArN→O cytotoxicity (Equation (3), Table 5) resulted in r^2 values close to those in previously obtained log (cytotoxicity) vs. E^1_7 relationships [31]. On the other hand, the use of a large group of ArN→O with highly variable and reduction potential-independent reactivity towards NQO1 (Table 2), enabled us to characterize the role of this enzyme in their cytotoxicity.

In regards to the possible mechanism of reduction of ArN→O by NQO1, one may note their structural similarity with 1,4-naphthoquinones, which are planar bicyclic molecules with similar electron self-exchange rate constants, ~10^8 M^{-1} s^{-1} [22,39]. The available data on the mechanism of quinone reduction are summarized below: (i) a net two-electron reduction of quinones by NQO1 is attributed to low stability of its FAD semiquinone (FAD^-), 8% under equilibrium [40], and the efficient electronic coupling, which is provided by the sandwiching of quinone ring between isoalloxazine ring

of FAD and Phe-178′ [41]; (ii) The instability of FAD^- does not restrict the reactivity of NQO1 with single-electron acceptors [19]. NQO1 reduces nitroaromatic compound tetryl in a mixed single- and two-electron way [42], and its reactions with quinones may be described by a multistep (e^-,H^+,e^-) hydride transfer model [19]; (iii) The reactivity of quinones roughly increases with their E17 and sharply decreases when their VdWvol is above 200 $Å^3$ [19]. An increase in VdWvol may increase the distance between N5 of isoalloxazine and quinone ring [43], and (iv) The $\Delta S^{\neq}$ values of 'fast' quinone oxidants with VdWvol ≤ 200 $Å^3$ are lower than $\Delta S^{\neq}$ of 'slow' quinones (VdWvol > 200 $Å^3$) by 40–70 J mol^{-1} K^{-1} [19]. More negative $\Delta S^{\neq}$ values point to the stronger electronic coupling between the molecules of reactants [44].

In our case, NQO1 reduces ArN→O 10^2–10^3 times slower than 1,4-naphthoquinones with comparable E^1_7 and VdWvol values, −0.36–−0.46 V, and 180–200 $Å^3$, respectively [19]. The use of a relatively fast NQO1 substrate, 3-CH_3CONH-1,2,4-benzotriazine-1,4-dioxide (**2**) (Table 2, Figure 2A,B), enabled the characterization of this process more thoroughly. The SOD-sensitive reduction of added cytochrome *c* during the reaction (Figure 2B) points to the formation of a free radical ((**b**), Scheme 1), which enters the redox equilibrium with O_2/O_2^- couple. In our opinion, the lower rate of ArN→O reduction when compared to quinones and the dissociation of free radicals may be caused by a weak electronic coupling of reactants. The electronic coupling may be weakened by the loss of planarity of (**b**) due to the adoption of markedly pyramidal geometries of N1 and N4 in a free radical state [45]. This is supported by $\Delta S^{\neq}$ value of 3-CH_3CONH-1,2,4-benzotriazine-1,4-dioxide, -43 J mol^{-1} K^{-1}, which is far less negative than $\Delta S^{\neq}$ of 'fast' quinone oxidants, −85–−75 J mol^{-1} K^{-1} [19]. However, the yield of free radicals in NQO1-catalyzed reduction of this compound, expressed as the ratio of cytochrome *c* reduction and doubled NADPH oxidation rates [27], is close to 30% (Figure 2B). This is much lower than the single-electron flux of 90–95%, observed in the reaction with single-electron transferring *Pf*FNR. In parallel, 3-CH_3CONH-1,2,4-benzotriazine-1,4-dioxide disappears in the course of the reaction (Figure 2A,B). Analogous although relatively slower process takes place during the reduction of TPZ by NQO1 [22]. The sum of this reaction rate and the halved rate of cytochrome *c* reduction is close to the total rate of NADPH oxidation (Figure 2B). The disappearance of oxidant is not caused by free radical dismutation, because its rate exhibits a linear, but not a square dependence on the enzyme concentration that is characteristic for the dismutation-driven process [46]. Thus, the possible explanation is that NQO1 performs mixed single- and two-electron reduction of ArN→O with the initial single-electron transfer step. The elucidation of the mechanism of a second electron transfer is more problematic because of debates whether the 1,4-dioxide (**a**) reduction product, 1-monoxide (**d**), is formed from free radical (**b**) directly, or via aryl radical (**c**) (Scheme 1) [2,7–11]. This problem is an object of our future studies, together with the detailed characterization of the reaction product(s).

The multiparameter regression analysis (Equation (3), Tables 3 and 5) provides the first quantitative confirmation of NQO1 contribution to the cytotoxicity of ArN→O in two cell lines. Given the data currently available, the most credible mechanism of their action is NQO1-catalyzed redox cycling. Apart from MH22a cells (Table 4), dicoumarol protected against TPZ aerobic cytotoxicity in A549 cells, besides, the TPZ-resistant A549 subline almost completely lost NQO1 activity [24]. On the other hand, there also exist data on the absence of the relationship between the content of NQO1 and the cytotoxicity of TPZ in several cell lines [23,25]. Because P-450R and/or nuclear reductases typically play the most significant role in the bioactivation of TPZ [16,17], it is possible that in certain cases their action may shield the role of NQO1. One may also expect that the role of NQO1 may be more expressed using its substrates more efficient than TPZ and especially possessing lower E^1_7 values, i.e., lower reactivity towards P-450R (Tables 1 and 2). In conclusion, our data indicate that NQO1 may be an important target of ArN→O in the cell. The further studies of electron transfer mechanism and substrate specificity of these reactions may increase the variety of efficient therapeutic agents of this group, and contribute to the optimization of their action.

4. Materials and Methods

4.1. Enzymes and Chemicals

Recombinant rat P-450R was a generous gift of Dr. Alexey Yantsevich (Institute of Bioorganic Chemistry, NAS of Belarus, Minsk, Belarus), and was prepared as described in [47]. Recombinant *P. falciparum* ferredoxin:$NADP^+$ oxidoreductase (*Pf*FNR) was a generous gift of Professor Alessandro Aliverti (Department of Biosciences, Universita degli Studi di Milano, Milano, Italy), and was prepared as previously described in [48]. NQO1 was prepared from rat liver according to Prochaska [49]. The enzyme concentrations were determined spectrophotometrically according to ε_{456} = 21.4 $mM^{-1}{\cdot}cm^{-1}$ (P-450R [47]), ε_{454} = 10.0 $mM^{-1}{\cdot}cm^{-1}$ (PfFNR [48]), and ε_{460} = 11.0 $mM^{-1}{\cdot}cm^{-1}$ (NQO1 [49]). Derivatives of tirapazamine (**1–5**) (Figure 1) were synthesized as described in [31,50]. Quinoxaline-1,4-dioxide and its derivatives (**6**,**7**) (Figure 1) were synthesized as described in [51,52]. 1,2,4-Benzotriazine-1,4-dioxide and derivatives of 1,2,4-benzotriazine-1-oxide (**8**,**9**) (Figure 1) were synthesized as described in [53,54]. The compound purity was characterized by IR and NMR spectrometry, melting point, and elemental analysis. NADPH, cytochrome *c*, superoxide dismutase, and other reagents were obtained from Sigma-Aldrich (St. Louis, MO, USA), and used as received.

4.2. Enzymatic Assays

The kinetic measurements were carried out spectrophotometrically using a PerkinElmer Lambda 25 spectrophotometer (PerkinElmer, Waltham, MA, USA) in 0.1 M K-phosphate buffer (pH 7.0) containing 1 mM EDTA at 25 °C. The enzyme activities determined according to the rate of reduction of 50 μM cytochrome *c* ($\Delta\varepsilon_{550}$ = 20 $mM^{-1}{\cdot}cm^{-1}$) at substrate concentrations indicated below were close to those reported previously [22]: 39 s^{-1} (P-450R, [NADPH] = 100 μM), and 1750 s^{-1} (NQO1, [NADPH] = 150 μM, [menadione] = 10 μM). In this case, 0.01% Tween 20 and 0.25 mg/mL bovine serum albumin were added as NQO1 activators. The activity of *Pf*FNR, determined according to the reduction rate of 1.0 mM ferricyanide ($\Delta\varepsilon_{420}$ = 1.03 $mM^{-1}{\cdot}cm^{-1}$) at [NADPH] = 100 μM was equal to 48 s^{-1}. The initial rates of P-450R- or *Pf*FNR-catalyzed NADPH-dependent *N*-oxide reduction were determined according to $\Delta\varepsilon_{340}$ = 6.2 $mM^{-1}{\cdot}cm^{-1}$ after the subtraction of intrinsic NADPH oxidase activities of enzymes, 0.05 s^{-1} (P-450R), and 0.1 s^{-1} (*Pf*FNR). The stock solutions of oxidants were prepared in DMSO (dilution factor 100). The initial rates of NQO1-catalyzed ArN→O reduction were determined according to the rate of NADPH oxidation. In this case, the rates were corrected for 340 nm absorbance changes due to ArN→O disappearance. The latter were obtained under the same conditions in the presence of NADPH regeneration system, 10 mM glucose-6-phosphate and 0.3 mg/mL glucose-6-phosphate dehydrogenase. The loss of 3-CH_3CONH-1,2,4-benzotriazine-1,4-dioxide during its reduction by NQO1 was monitored according to $\Delta\varepsilon_{427}$ = 6.45 $mM^{-1}{\cdot}cm^{-1}$, which was calculated according to the absorbance difference of compounds (**2**) and (**9**) (Figure 1). The values of turnover rate, k_{cat}, reflecting the maximal number of moles NADPH oxidized or oxidant reduced per mole of the enzyme active center per second, and k_{cat}/K_m, the bimolecular rate constant (or catalytic efficiency constant), corresponds to the inverse intercepts and slopes in Lineweaver-Burk coordinates, [E]/*v* vs. 1/[oxidant]. These rate constants were obtained by fitting the experimental data to the parabolic expression using the SigmaPlot 2000 (version 11.0, Systal Software, San Jose, CA, USA). The temperature dependence of reaction rate was examined at seven fixed temperatures between 15 and 45 °C in the absence of activators, the activation enthalpies and entropies of reaction were calculated from Eyring plots of ln (k_{cat}/K_m)/T vs. 1/T.

4.3. Cytotoxicity Assays

Murine hepatoma MH22a cells obtained from the Institute of Cytology of the Russian Academy of Sciences (St. Petersburg, Russia), were grown and maintained at 37 °C in DMEM medium, supplemented with 10% fetal bovine serum, 100 U/mL penicillin, and 0.1 mg/mL streptomycin, as described in [22]. In the cytotoxicity experiments, 3.0×10^4/mL cells were seeded in 5-mL flasks

either in the presence or in the absence of compounds and were grown for 24 h. In the absence of compounds, cells reached 40–50% confluence. The adherent cells were counted under a light microscope. Typically, they did not accumulate Trypan blue and their viability was 98.5–99.3%. Human colon adenocarcinoma cells HCT-116 obtained from ATCC (Manassas, VA, USA), were grown and maintained at 37 °C in 5% CO_2 in RPMI 1640 DMEM medium, supplemented with 10% fetal bovine serum, 2 mM L-glutamine, and 0.05 mg/mL gentamycin. In the cytotoxicity experiments, 1.0×10^5/mL cells were seeded in the absence or the presence of compounds and were grown for 48 h. In the absence of compounds, cells reached 65–75% confluence. Their viability was determined by staining with crystal violet [55]. Stock solutions of compounds were prepared in DMSO. Its concentration in cultivation media did not exceed 0.2% and did not affect cell viability. The experiments were conducted in triplicate.

4.4. Statistical Analysis and Calculations

The statistical analysis was performed using Statistica (version 4.3, Statsoft, Toronto, ON, Canada). Octanol/water distribution coefficients at pH 7.0 (log *D*) were calculated using LogD Predictor (https://chemaxon.com).

Supplementary Materials: Supplementary materials can be found at http://www.mdpi.com/1422-0067/21/22/8754/s1.

Author Contributions: A.N.-Č. and V.J. performed the cytotoxicity studies, J.Š. synthesized compounds, L.M., A.M., and M.L. performed kinetic experiments and purified NQO1, N.Č. designed and supervised the experiments and wrote the manuscript. All authors have read and agreed to the published version of the manuscript.

Funding: This work was supported by the European Social Fund (Measure No. 09.33-LMT-K-712, grant No. DOTSUT-34/09.3.3.-LMT-K712-01-0058/LSS-600000-58).

Acknowledgments: We thank Alexey Yantsevich and Alesandro Aliverti for their generous gift of purified P-450R and *Pf*FNR, respectively, and Valė Miliukienė (Institute of Biochemistry) for mice splenocyte cytotoxicity studies.

Conflicts of Interest: The authors declare no conflict of interest.

Abbreviations

ArN→O	Heteroaromatic *N*-oxide
BCNU	1,3-bis(2-chloroethyl)-1-nitrosourea
cL_{50}	Concentration for 50% cell survival
DESF	Desferrioxamine
DIC	Dicoumarol
DPPD	*N*,*N*′-diphenyl-*p*-phenylene diamine
E^1_7	Single-electron reduction midpoint potential at pH 7.0
GI_{50}	Concentration for 50% inhibition of maximal cell proliferation
k_{cat}	Catalytic constant
k_{cat}/K_m	Bimolecular rate constant
k_{cat}/K_m (avge)	Geometric average of k_{cat}/K_m in P-450R- and *Pf*FNR-catalyzed reactions
k_{cat}/K_m (NQO1)	k_{cat}/K_m in NQO1-catalyzed reaction
log *D*	Octanol/water distribution coefficient at pH 7.0
NQO1	NAD(P)H:quinone oxidoreductase
P-450R	NADPH:cytochrome P-450 reductase
*Pf*FNR	*Plasmodium falciparum* ferredoxin:$NADP^+$ oxidoreductase
SOD	Superoxide dismutase
TPZ	Tirapazamine

References

1. Wardman, P.; Dennis, M.F.; Everett, S.A.; Patel, K.B.; Stratford, M.R.L.; Tracy, M. Radicals from one-electron reduction of nitro compounds, aromatic *N*-oxides and quinones: The kinetic basis for hypoxia-selective, bioreductive drugs. *Biochem. Soc. Symp.* **1995**, *61*, 171–194. [PubMed]
2. Shen, X.; Gates, K.S. Enzyme-activated generation of reactive oxygen species from heterocyclic *N*-oxides under aerobic and anaerobic conditions and its relevance to hypoxia-selective prodrugs. *Chem. Res. Toxicol.* **2019**, *32*, 348–361. [CrossRef] [PubMed]
3. Shah, Z.; Mahnuba, R.; Turcotte, B. The anticancer drug tirapazamine has antimicrobial activity against *Escherichia coli*, *Staphylococcus aureus* and *Clostridium difficile*. *FEMS Microbiol. Lett.* **2013**, *347*, 61–69. [CrossRef] [PubMed]
4. Gil, A.; Pabon, A.; Galiano, S.; Burguete, A.; Perez-Silanes, S.; Deharo, E.; Monge, A.; Aldana, I. Synthesis, biological evaluation and structure-activity relationships of new quinoxaline derivatives as anti-*Plasmodium falciparum* agents. *Molecules* **2014**, *19*, 2166–2180. [CrossRef]
5. Cheng, G.; Li, B.; Wang, C.; Zhang, H.; Liang, G.; Weng, Z.; Hao, H.; Wang, X.; Liu, Z.; Dai, M.; et al. Systematic and molecular basis of the antibacterial action of quinoxaline 1,4-di-*N*-oxides against *Escherichia coli*. *PLoS ONE* **2015**, *10*, e0136450. [CrossRef]
6. Perez-Silanes, S.; Torrers, E.; Arbillaga, L.; Varela, J.; Cerecetto, H.; Gonzalez, M.; Azqueta, A.; Moreno-Viguri, E. Synthesis and biological evaluation of quinoxaline di-*N*-oxide derivatives with *in vitro* trypanocidal activity. *Bioorg. Med. Chem. Lett.* **2016**, *26*, 903–906. [CrossRef]
7. Shen, X.; Rajapakse, A.; Galazzi, F.; Junnotula, V.; Fuchs-Knotts, T.; Glaser, R.; Gates, K.S. Isotopic labeling experiments that elucidate the mechanism of DNA strand cleavage by the hypoxia-selective antitumor agent 1,2,4-benzotriazine 1,4-di-*N*-oxide. *Chem. Res. Toxicol.* **2013**, *22*, 111–118. [CrossRef]
8. Yadav, P.; Marshall, A.J.; Reynisson, J.; Denny, W.A.; Hay, M.P.; Anderson, R.F. Fragmentation of the quinoxaline *N*-oxide bond to the ·OH radical upon one-electron bioreduction. *Chem. Commun.* **2014**, *50*, 13729–13731. [CrossRef]
9. Shinde, S.S.; Maroz, A.; Hay, M.P.; Patterson, A.V.; Denny, V.A.; Anderson, R.F. Characterization of radicals formed following enzymatic reduction of 3-substituted analogues of the hypoxia-selective cytotoxin 3-amino-1,2,4-benzotriazine 1,4-dioxide (tirapazamine). *J. Am. Chem. Soc.* **2010**, *132*, 2591–2599. [CrossRef]
10. Anderson, R.F.; Yadav, P.; Shinde, S.S.; Hong, C.R.; Pullen, S.M.; Reynisson, J.; Wilson, W.R.; Hay, M.P. Radical chemistry and cytotoxicity of bioreductive 3-substituted quinoxaline di-*N*-oxides. *Chem. Res. Toxicol.* **2016**, *29*, 1310–1324. [CrossRef]
11. Fuchs, T.; Chowdhury, G.; Fuchs, C.L.; Gates, K.S. 3-Amino-1,2,4-benzotriazine 4-oxide: Characterization of a new metabolite arising from bioreductive processing of the antitumour agent 3-amino-1,2,4-benzotriazine 1,4-dioxide (tirapazamine). *J. Org. Chem.* **2001**, *66*, 107–114. [CrossRef] [PubMed]
12. Zarranz, B.; Jaso, A.; Aldana, I.; Monge, A. Synthesis and anticancer activity evaluation of new 2-alkylcarbonyl and 2-benzoyl-1-trifluoromethyl-quinoxaline-1,4-di-*N*-oxide derivatives. *Bioorg. Med. Chem.* **2004**, *12*, 3711–3721. [CrossRef] [PubMed]
13. Hu, Y.; Xia, Q.; Shangguan, S.; Liu, X.; Hu, Y.; Sheng, R. Synthesis and biological evaluation of 3-aryl-quinoxaline-2-carbonitrile 1,4-di-*N*-oxide derivatives as hypoxic selective anti-tumour agents. *Molecules* **2012**, *17*, 9683–9696. [CrossRef] [PubMed]
14. Chowdhury, G.; Sarkar, U.; Pullen, S.; Wilson, W.R.; Rajapakse, A.; Fuchs-Knotts, T.; Dates, K.S. DNA strand cleavage by the phenazine di-*N*-oxide natural product myxin under both aerobic and anaerobic conditions. *Chem. Res. Toxicol.* **2012**, *25*, 197–206. [CrossRef]
15. Gu, Y.; Chang, T.T.-A.; Wang, J.; Jaiswal, J.K.; Edwards, D.; Downes, N.J.; Liyanage, H.D.S.; Lynch, C.H.R.; Pruijn, F.B.; Hickey, A.J.R.; et al. Reductive metabolism influences the toxicity and pharmacokinetics of the hypoxia-targeted benzotriazine-dioxide anticancer agent SN30000 in mice. *Front. Pharmacol.* **2017**, *8*, 531. [CrossRef]
16. Hunter, F.W.; Young, R.J.; Shalev, Z.; Vellanki, R.N.; Wang, J.; Gu, Y.; Joshi, N.; Sreebhavan, S.; Weinreb, J.; Goldstein, D.P.; et al. Identification of P450 oxidoreductase as a major determinant of sensitivity to hypoxia-activated prodrugs. *Cancer Res.* **2015**, *75*, 4211–4223. [CrossRef]
17. Delahussaye, Y.M.; Evans, J.W.; Brown, J.M. Metabolism of tirapazamine by multiple reductases in the nucleus. *Biochem. Pharmacol.* **2001**, *62*, 1201–1209.

18. Ross, D.; Siegel, D. NAD(P)H:quinone oxidoreductase I (NQO1, DT-diaphorase), functions and pharmacogenetics. *Meth. Enzymol.* **2004**, *382B*, 115–144.
19. Anusevičius, Ž.; Šarlauskas, J.; Čėnas, N. Two-electron reduction of quinones by rat liver NAD(P)H: Quinone oxidoreductase: Quantitative structure-activity relationships. *Arch. Biochem. Biophys.* **2002**, *404*, 254–262. [CrossRef]
20. Misevičienė, L.; Anusevičius, Ž.; Šarlauskas, J.; Čėnas, N. Reduction of nitroaromatic compounds by NAD(P)H:quinone oxidoreductase (NQO1): The role of electron-accepting potency and structural parameters in the substrate specificity. *Acta Biochim. Pol.* **2006**, *53*, 569–576. [CrossRef]
21. Di Francesco, A.; Ward, T.; Butler, J. Diaziridinylbenzoquinones. *Meth. Enzymol.* **2004**, *382B*, 174–193.
22. Nemeikaitė-Čėnienė, A.; Šarlauskas, J.; Jonušienė, V.; Marozienė, A.; Misevičienė, L.; Yantsevich, A.V.; Čėnas, N. Kinetics of flavoenzyme-catalyzed reduction of tirapazamine derivatives: Implications for their prooxidant cytotoxicity. *Int. J. Mol. Sci.* **2019**, *20*, 4602. [CrossRef] [PubMed]
23. Plumb, J.A.; Gerritsen, M.; Workman, P. DT-diaphorase protects cells from the hypoxic cytotoxicity of indoloquinone EO9. *Br. J. Cancer* **1994**, *70*, 1136–1143. [CrossRef] [PubMed]
24. Elwell, J.H.; Siim, B.G.; Evans, J.W.; Brown, J.M. Adaptation of human tumour cells to tirapazamine under aerobic conditions. Implications of increased antioxidant enzyme activity to mechanism of aerobic toxicity. *Biochem. Pharmacol.* **1997**, *54*, 249–257. [CrossRef]
25. Sharp, S.Y.; Kelland, L.R.; Valenti, M.R.; Brunton, L.A.; Hobbs, S.; Workman, P. Establishment of an isogenic human colon tumor model for NQO1 gene expression: Application to investigate the role of DT-diaphorase in bioreductive drug activation in vitro and in vivo. *Mol. Pharmacol.* **2000**, *58*, 1146–1155. [CrossRef]
26. Beaver, S.K.; Mesa-Tores, N.; Pey, A.L.; Timson, D.J. NQO1: A target for the treatment of cancer and neurological diseases, and a model to understand loss of function disease mechanism. *Biochim. Biophys. Acta Proteins Proteom.* **2019**, *1867*, 663–676. [CrossRef]
27. Lesanavičius, M.; Aliverti, A.; Šarlauskas, J.; Čėnas, N. Reactions of *Plasmodium falciparum* ferredoxin: $NADP^+$ oxidoreductase with redox cycling xenobiotics: A mechanistic study. *Int. J. Mol. Sci.* **2020**, *21*, 3234. [CrossRef]
28. Marcus, R.A.; Sutin, N. Electron transfers in chemistry and biology. *Biochim. Biophys. Acta* **1985**, *811*, 265–322. [CrossRef]
29. Čėnas, N.; Nemeikaitė-Čėnienė, A.; Sergedienė, E.; Nivinskas, H.; Anusevičius, Ž.; Šarlauskas, J. Quantitative structure-activity relationships in enzymatic single-electron reduction of nitroaromatic explosives: Implications for their cytotoxicity. *Biochim. Biophys. Acta* **2001**, *1528*, 31–38. [CrossRef]
30. Šarlauskas, J.; Nivinskas, H.; Anusevičius, Ž.; Misevičienė, L.; Marozienė, A.; Čėnas, N. Estimation of single-electron reduction potentials (E^1_7) of nitroaromatic compounds according to the kinetics of their single-electron reduction by flavoenzymes. *Chemija* **2006**, *17*, 31–37.
31. Hay, M.P.; Gamage, S.A.; Kovacs, M.S.; Pruijn, F.B.; Anderson, R.F.; Patterson, A.V.; Wilson, W.R.; Brown, J.M.; Denny, W.A. Structure-activity relationships of 1,2,4-benzotriazine 1,4-dioxides as hypoxia-selective analogues of tirapazamine. *J. Med. Chem.* **2003**, *46*, 169–182. [CrossRef] [PubMed]
32. Anderson, R.F.; Shinde, S.S.; Hay, M.P.; Denny, W.A. Potentiation of the cytotoxicity of the anticancer agent tirapazamine by benzotriazine-*N*-oxides. The role of redox equilibria. *J. Am. Chem. Soc.* **2006**, *128*, 245–249. [CrossRef] [PubMed]
33. Cahill, A.; Jenkins, T.C.; White, I.N.H. Metabolism of 3-amino-1,2,4-benzotriazine-1,4-dioxide (SR 4233) by purified DT-diaphorase under aerobic and anaerobic conditions. *Biochem. Pharmacol.* **1993**, *45*, 321–329. [CrossRef]
34. Zhao, Y.H.; Abraham, M.H.; Zissimos, A.M. Fast calculation of van der Waals volume as a sum of atomic and bond contributions and its application to drug compounds. *J. Org. Chem.* **2003**, *68*, 7368–7373. [CrossRef]
35. Öllinger, K.; Brunmark, A. Effects of hydroxyl substituent position on 1,4-naphthoquinone toxicity to rat hepatocytes. *J. Biol. Chem.* **1991**, *266*, 21496–21503.
36. Nemeikaitė, A.; Čėnas, N. The changes of prooxidant and antioxidant enzyme activities in bovine leukemia virus-transformed cells. Their influence on quinone cytotoxicity. *FEBS Lett.* **1993**, *326*, 65–68. [CrossRef]
37. Liu, C.-H.; Chiu, T.-Y.; Hu, M.-L. Fucoxanthin enhances HO-1 and NQO1 expression in murine hepatic BNL CL.2 cells through activation of the Nrf2/ARE system partially by its prooxidant activity. *J. Agric. Food Chem.* **2011**, *59*, 11344–11351. [CrossRef]

38. Miliukienė, V.; Nivinskas, H.; Čėnas, N. Cytotoxicity of anticancer aziridinyl-substituted benzoquinones in primary mice splenocytes. *Acta Biochim. Pol.* **2014**, *61*, 833–836. [CrossRef]
39. Grampp, G.; Jaenicke, W. ESR-spectroscopic investigation of the parallel electron and proton exchange between quinones and their radicals: Part I. Measurements at 298 K. *J. Electroanal. Chem.* **1987**, *229*, 297–303. [CrossRef]
40. Tedeschi, G.; Chen, S.; Massey, V. DT-diaphorase. Redox potential, steady-state, and rapid reaction studies. *J. Biol. Chem.* **1995**, *270*, 1198–1204. [CrossRef]
41. Faig, M.; Bianchet, M.A.; Talalay, P.; Chen, S.; Winski, S.; Ross, D.; Amzel, L.M. Structures of recombinant human and mouse NAD(P)H:quinone oxidoreductases: Species comparison and structural changes with substrate binding and release. *Proc. Natl. Acad. Sci. USA* **2000**, *97*, 3177–3182. [CrossRef] [PubMed]
42. Anusevičius, Ž.; Šarlauskas, J.; Nivinskas, H.; Segura-Aguilar, J.; Čėnas, N. DT-diaphorase catalyzes *N*-denitration and redox cycling of tetryl. *FEBS Lett.* **1998**, *436*, 144–148. [CrossRef]
43. Mendoza, M.F.; Hollabaugh, N.M.; Hettiarachchi, S.U.; McCarley, R.L. Human NAD(P)H: Quinone oxidoreductase type I (hNQO1) activation of quinone propionic acid trigger groups. *Biochemistry* **2012**, *51*, 8014–8026. [CrossRef] [PubMed]
44. Hubig, S.M.; Rathore, R.; Kochi, J.K. Steric control of electron transfer. Changeover from outer-sphere to inner-sphere mechanism in arene/quinone redox pairs. *J. Am. Chem. Soc.* **1999**, *121*, 617–626. [CrossRef]
45. Yin, J.; Glaser, R.; Gates, K.S. Electron and spin-density analysis of tirapazamine reduction chemistry. *Chem. Res. Toxicol.* **2012**, *25*, 620–633. [CrossRef] [PubMed]
46. Holzman, J.L.; Crankshaw, D.L.; Peterson, F.J.; Polnaszek, C.F. The kinetics of the aerobic reduction of nitrofurantoin by NADPH-cytochrome P450 (*c*) reductase. *Mol. Pharmacol.* **1981**, *20*, 669–673.
47. Pechurskaja, T.A.; Harnastai, I.N.; Grabovec, I.P.; Gilep, A.A.; Usanov, S.A. Adrenodoxin supports reactions catalyzed by microsomal steroidgenetic cytochrome P450s. *Biochem. Biophys. Res. Commun.* **2007**, *353*, 598–604. [CrossRef]
48. Balconi, E.; Pennati, A.; Crobu, D.; Pandini, V.; Cerutti, R.; Zanetti, G.; Aliverti, A. The ferredoxin-$NADP^+$ reductase/ferredoxin electron transfer system of *Plasmodium falciparum*. *FEBS J.* **2009**, *276*, 2249–4260. [CrossRef]
49. Prochaska, H.J. Purification and crystallization of rat liver NAD(P)H:quinone-acceptor oxidoreductase by cibacron blue affinity chromatography: Identification of a new and potent inhibitor. *Arch. Biochem. Biophys.* **1988**, *267*, 529–538. [CrossRef]
50. Polmickaitė-Smirnova, E.; Šarlauskas, J.; Krikštopaitis, K.; Lukšienė, Ž.; Staniulytė, Z.; Anusevičius, Ž. Preliminary investigation on the antibacterial activity of antitumor drug 3-amino-1,2,4-benzotriazine-1,4-dioxide (tirapazamine) and its derivatives. *Appl. Sci.* **2020**, *10*, 4062. [CrossRef]
51. Abushanab, E. Long-range hydrogen-fluorine spin-spin coupling. Further support for the "through-space" (direct) mechanism. *J. Am. Chem. Soc.* **1971**, *93*, 6532–6536. [CrossRef]
52. Monge, A.; Palop, J.A.; Del Castillo, J.C.; Caldero, J.M.; Roca, J.; Romero, G.; Del Rio, J.; Lasheras, B. Novel antagonists of 5-HT_3 receptors: Synthesis and biological evaluation of piperazinylquinoxaline derivatives. *J. Med. Chem.* **1993**, *36*, 2745–2750. [CrossRef] [PubMed]
53. Robbins, R.F.; Schofield, K. Polyazabicyclic compounds. Part II. Further derivatives of benzo-1:2:4-triazine. *J. Chem. Soc.* **1957**, 3186–3194. [CrossRef]
54. Bodzioch, A.; Pomiklo, D.; Celeda, M.; Pietrzak, A.; Kaszynski, P. 3-Substituted benzo[e][1,2,4]triazines: Synthesis and electronic effects of the C(3) substituents. *J. Org. Chem.* **2019**, *84*, 6377–6394. [CrossRef]
55. Ito, M. Microassay for studying anticellular effects of human interferons. *J. Interferon. Res.* **1984**, *4*, 603–608. [CrossRef] [PubMed]